

D. Dodt, M. Brix, M.N.A. Beurskens, J. Flannagan, M Kempnaars,  
M. Maslov, R. Fischer, J. Schweinzer, S. Zoletnik, D. Dunai, S. Nedzelskiy,  
D. Refy, G. Petravich, M.J. Leyland and JET EFDA contributors

# Pedestal Density Profiles from the Upgraded Lithium Beam Diagnostic at JET and Comparison to Expectations from Neutral Penetration

“This document is intended for publication in the open literature. It is made available on the understanding that it may not be further circulated and extracts or references may not be published prior to publication of the original when applicable, or without the consent of the Publications Officer, EFDA, Culham Science Centre, Abingdon, Oxon, OX14 3DB, UK.”

“Enquiries about Copyright and reproduction should be addressed to the Publications Officer, EFDA, Culham Science Centre, Abingdon, Oxon, OX14 3DB, UK.”

The contents of this preprint and all other JET EFDA Preprints and Conference Papers are available to view online free at [www.iop.org/Jet](http://www.iop.org/Jet). This site has full search facilities and e-mail alert options. The diagrams contained within the PDFs on this site are hyperlinked from the year 1996 onwards.

# Pedestal Density Profiles from the Upgraded Lithium Beam Diagnostic at JET and Comparison to Expectations from Neutral Penetration

D. Dodt<sup>1</sup>, M. Brix<sup>2</sup>, M.N.A. Beurskens<sup>2</sup>, J. Flannagan<sup>2</sup>, M Kempnaars<sup>2</sup>, M. Maslov<sup>3</sup>, R. Fischer<sup>1</sup>, J. Schweinzer<sup>1</sup>, S. Zoletnik<sup>4</sup>, D. Dunai<sup>4</sup>, S. Nedzelskiy<sup>5</sup>, D. Refy<sup>4</sup>, G. Petravich<sup>4</sup>, M.J. Leyland<sup>6</sup> and JET EFDA contributors\*

*JET-EFDA, Culham Science Centre, OX14 3DB, Abingdon, UK*

<sup>1</sup>*Max-Planck-Institut für Plasmaphysik, EURATOM Association, D-85748 Garching, Germany*

<sup>2</sup>*EURATOM-CCFE Fusion Association, Culham Science Centre, OX14 3DB, Abingdon, OXON, UK*

<sup>3</sup>*Ecole Polytechnique Fédérale de Lausanne (EPFL)*

<sup>4</sup>*KFKI RMKI, EURATOM Association, Budapest, Hungary*

<sup>5</sup>*Association EURATOM/IST, Inst. Superior Técnico, Lisboa, Portugal*

<sup>6</sup>*York Plasma Institute, Department of Physics, University of York, Heslington, York, YO10 5DD, UK*

\* *See annex of F. Romanelli et al, "Overview of JET Results", (23rd IAEA Fusion Energy Conference, Daejeon, Republic of Korea (2010)).*



## INTRODUCTION

The lithium beam diagnostic at JET provides information about the electron density in the scrape-off-layer and pedestal region. The density is reconstructed from the spatial profile of the 2p line emission of a collisionally excited neutral lithium beam (energy typically 60keV), which is injected into the plasma edge from the top of the machine parallel to the direction of the Z coordinate. The spatial and temporal resolution achieved at JET is  $\Delta t \approx 10\text{ms}$ ,  $\Delta Z \approx 1\text{cm}$ . The beam emission is observed using a periscope [1]. The reconstruction uses a probabilistic inversion procedure which is based on a collisional-radiative model for the beam-plasma interaction [2].

### 1. APPARATUS FUNCTION OF THE OBSERVATION PERISCOPE

The diagnostic model was extended by a description of the spatial averaging of the beam emission caused by the finite resolution of the beam periscope. Without a detailed description of the apparatus function of the imaging periscope, an overshooting of the reconstructed density was observed for profiles with very steep density pedestal. For a local beam emission of the form  $\varepsilon(R, Z, \Phi) = \varepsilon(Z) s(R, \Phi)$ , where  $\varepsilon(Z)$  is given by the collisional radiative model and  $s(R, \Phi)$  is the transversal beam current distribution, the intensity  $I_i$  observed by channel  $i$  is proportional to (line of sight volume  $V_i$ )

$$I_i \propto \int_{V_i} \varepsilon(R, Z, \Phi) dR dZ d\Phi = \int_{Z_0}^{Z_1} \varepsilon(Z') \underbrace{\int_{A(Z')} s(R, \Phi) dR d\Phi}_{w_i(x')} dZ', \quad (1)$$

where the transformed coordinate  $Z' = Z + f(R)$  is chosen to take into account the shape of flux surfaces, which is not perpendicular to the injected beam. Note that the Jacobi determinant of the transformed coordinates equals one for this transformation.  $f(R)$  is the approximate deviation of the flux surfaces from the perpendicular plane (compare Figure 1). The one dimensional beam emission model is convoluted with the weight function  $w(Z)$  to take into account the spatial averaging.  $w(Z)$  is computed numerically for each pulse depending on the adjustable angle of the observation  $\alpha$  (typically up to  $30^\circ$ ). The improved model allows the inversion of beam emission profiles even for steep density pedestals. The resolution capabilities of the lithium beam diagnostic were studied using simulated data. Density profiles with pedestal widths of 1cm at the mid-plane can be successfully reconstructed using the improved model.

### 2. COMBINED FIT WITH DATA FROM HIGH RESOLUTION THOMSON SCATTERING

The data from the lithium beam diagnostic, which provides information about the plasma edge (scrape-off-layer and pedestal) is combined with data from the High Resolution Thomson Scattering system (HRTS), providing reliable information about the plasma core and top of the pedestal region. Note that the data from the two diagnostics don't have to be spatially shifted for the analysis. It was shown using a set of steady state L-Mode phases, in which the smoother pedestal region allows to assess spatial offsets between both diagnostics, that both systems agree to within 1.2cm. Since

HRTS data is only taken into account in the pedestal top region, where the profile is relatively flat, a shift of that magnitude has a negligible influence on the profile.

The combined profiles from HRTS and lithium beam have been fitted using a modified tanh function to extract parameters characterizing the pedestal region, i.e. width and height as well as the density at the pedestal foot:

$$n_e(R') = n_{e,sol} + 0.5 \cdot (n_{e,ped} - n_{e,sol}) \cdot \left( \frac{e^{R'(1 + R' s_{ped})} - e^{-R'(1 + R' s_{sol})}}{e^{R'} + e^{-R'}} + 1 \right) \quad (2)$$

where  $R'(R) := \frac{R - R_0}{2 \cdot w_{ne}}$  and  $R_0$  is the symmetry point of the tanh function,  $n_{e,ped}$  and  $n_{e,sol}$  are the densities at the pedestal top and foot and  $s_{ped}$  and  $s_{sol}$  are the slope of the density at the pedestal top and foot and  $w_{ne}$  is the pedestal width. See Figure 2 for an example. The results have been validated using different fit procedures as described by [5].

### 3. COMPARISON TO RESULTS FROM THE HIGH RESOLUTION THOMSON SCATTERING DIAGNOSTIC

The results have been compared to results obtained from ELM synchronized, averaged HRTS data obtained during a steady state phase (JET Pulse No: 79499,  $t = 18.5-22.5s$ ), see Figure 3. By looking at averaged profiles, the pedestal width can be extracted from the HRTS diagnostic alone and a steepening of the pedestal during the ELM cycle was reported [4] that can be confirmed with better time resolution using the Lithium beam data. A comparison to fits of data from fast sweeping reflectometry [3] performed for JET Pulse No: 79697 also showed good agreement.

### 4. TRENDS IN THE PEDESTAL WIDTH OF SELECTED PULSES

In Figure 4, the pedestal width and height are shown for a number of pulses. Two cluster can be identified in the data: L-Mode plasmas tend to show a wide pedestal at low pedestal top densities, while H-Mode plasmas typically have a steep pedestal and reach higher densities. Despite this general trend, some L-Mode plasmas have quite narrow pedestals at low densities. A neutral penetration model [6] predicts a pedestal width of

$$\Delta_{ne} = \frac{2V_n}{\langle \sigma_i v_e \rangle E n_{e,ped}}, \quad (3)$$

where  $V_n$  is the inward velocity of neutral hydrogen atoms perpendicular to the magnetic surface,  $\langle \sigma_i v_e \rangle$  is the ionization rate coefficient at separatrix conditions (density and temperature),  $E$  quantifies the effect of the variation of the flux surface distances at the positions of the fueling and the position where the profile is measured.

In order to assess  $V_n$ , Mahdavi et al. [6] assume a velocity distribution of the neutrals which is composed of two major contributions: Franck-Condon neutrals with temperatures 3eV and those that have charge-exchanged with plasma ions and have a temperature like the ions at the last closed

flux surface. The band in Figure 4 is obtained by assuming a Franck-Condon dominated neutral population, which gives a lower limit for the penetration of the neutrals. Especially at higher densities, the contribution from charge-exchange neutrals should broaden the pedestal width. A more accurate description of the neutral velocity can in principle be obtained using neutral fueling models but was not performed for this analysis.

The neutral penetration model correctly predicts the overall magnitude of the observed pedestal width. Without correction for the increase of the neutral velocity with rising densities, it predicts a narrowing of the pedestal as function of density. This agrees to some extent with the overall structure of the data showing two clusters of L- and H-mode plasmas, but does not describe the behaviour of the data within the two clusters or at high densities.

## REFERENCES

- [1]. M. Brix et al., Review of Scientific Instruments **81**, 10D733 (2010)
- [2]. D. Dodt et al., Proc. of the 36th EPS Plasma Phys. Sofia, 2009 ECA 33E, P-2.148 (2009)
- [3]. A. Sirinelli et al., Review of Scientific Instruments , **81**, 10D939 (2010)
- [4]. M. Beurskens et al., H-Mode workshop (2011); in prep. for Nuclear Fusion by M. Leyland
- [5]. P. Schneider et al., contrib. 13th Workshop on H-mode Phys. and Transp. Barriers (2011)
- [6]. M.A. Mahdavi et al., Physics of Plasmas **10**, 3984 (2003)

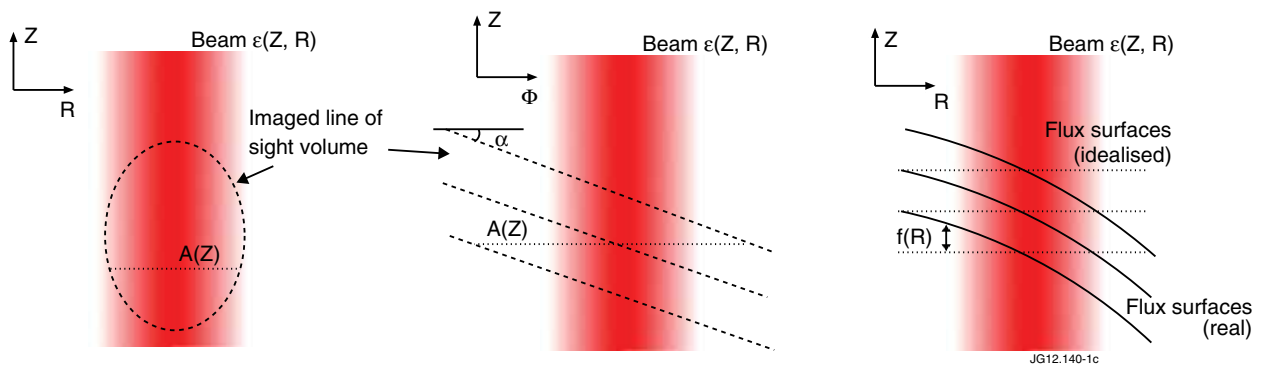


Figure 1: Spatial averaging of the optics and effect of non perpendicular flux surfaces, the beam width (FWHM) is typically 2cm.

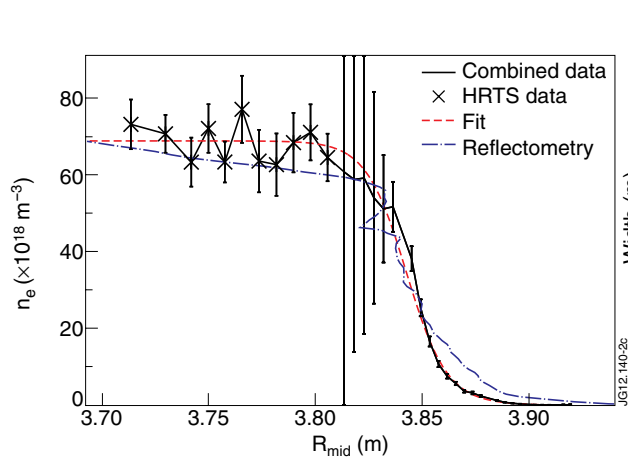


Figure 2: Fit of the combined density profile (JET Pulse Number JET Pulse No: 79697, time = 14.805s). The HRTS data points which complement the density profile at the pedestal top are marked using stars. The density profile from reflectometry is shown for comparison.

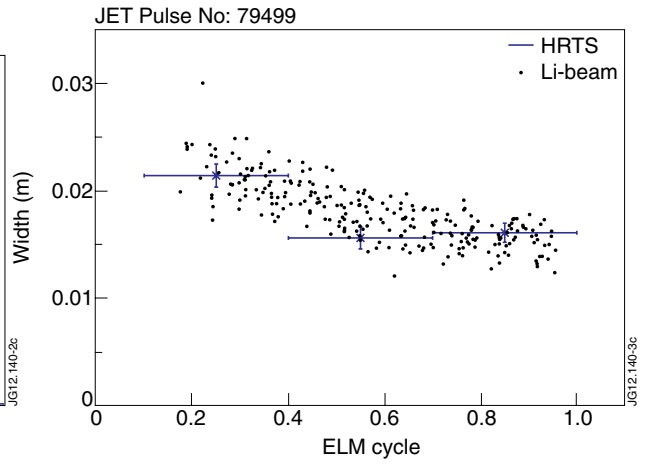


Figure 3: Comparison between pedestal width obtained by the Thomson scattering and the lithium beam diagnostic.

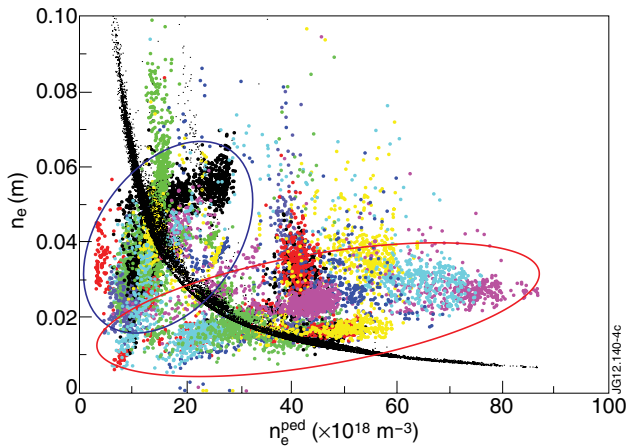


Figure 4: Pedestal width measured during a number of pulses as function of pedestal top density. The data from different pulses are shown in different colors. The black band following a  $1/n_{e,ped}$  dependence is the lower limit of the prediction of the model by Mahdavi et al. [6], the circles indicate the two clusters associated with L-Mode and H-Mode plasmas, respectively.